Analyst

Cite this: *Analyst*, 2012, **137**, 5607

www.rsc.org/analyst

PAPER

A sensitive strategy for label-free and time-resolved fluorescence assay of thrombin using Tb-complex and unmodified gold nanoparticles†

Dawei Huang,[a] Chenggang Niu,*[a] Zhizhang Li,[b] Min Ruan,[a] Xiaoyu Wang[a] and Guangming Zeng*[a]

Received 14th August 2012, Accepted 24th September 2012
DOI: 10.1039/c2an36117e

Gold nanoparticles (GNPs) can effectively differentiate the unfolded and folded aptamer, and quench the fluorescence of terbium ternary complexes (Tb-complexes), thus the authors herein report a sensitive strategy for protein detection, using label-free aptamer, Tb-complexes and GNPs. In the presence of thrombin, the aptamer is inclined to form G-quartet, and the folded aptamer cannot adsorb on the surface of GNPs, inducing the GNPs aggregation in the presence of 0.5 mol L^{-1} salt. After centrifugation at low speed to remove the aggregated GNPs, the quenching capability of the supernatant for Tb-complexes is decreased. The fluorescence intensity of Tb-complexes increases as the concentration of thrombin increases. Due to the highly specific recognition ability of the aptamer for thrombin and the strong quenching property of GNPs for Tb-complexes, the proposed protocol has good selectivity and high sensitivity for thrombin. Under the optimum conditions, a linear range from 1.0×10^{-9} M to 1.0×10^{-8} M is obtained with a detection limit of 0.14 nM, which is much lower than those commonly obtained for colorimetric sensors and some fluorescent sensors. The signal of Tb-complexes can be measured by time-resolved manner which made most of the unspecific fluorescent background signals be eliminated. The proposed sensor has been successfully applied in complicated biological samples for thrombin detection, and it can provide a promising potential for label-free aptamer-based protein detection.

1. Introduction

Aptamers, obtained from random-sequence nucleic acid libraries by an *in vitro* evolution process called SELEX, are single-strand nucleic acids with high specificity and affinity to many given targets ranging from small molecules to large proteins and even cells.[1–7] The aptamers have many merits, such as easy storage, excellent chemical stability and reproducibility, low cost and wide applicability.[8,9] There are three important reasons to explain the high affinity and specificity of aptamers toward targets, molecular shape complementarity, hydrogen-bonding interactions, and stacking interactions.[10] On the basis of the high affinity and specificity of aptamers toward targets, many researchers are particularly interested to develop aptamer-based sensors for targets detection. Highly sensitive and selective detection of proteins in complex biological media is very important for clinical diagnosis or research.[11–14] The optical methods based on aptamers are usually applied to the detection of proteins in complex biological media. In the presence of proteins, aptamers can form three dimensional aptamer–protein complexes, which make the aptamers have conformational changes, and importantly, these conformational changes can be transduced into optical signals, which can be monitored by apparatus.[15] There are two major kinds of optical methods to detect aptamer–protein interactions: colorimetric sensors[16–19] and fluorescent sensors.[14,20–22] The fluorescent sensors showed higher sensitivity compared to colorimetric sensors. However, in conventional fluorescent biosensors, there is a serious problem of how to eliminate background noises caused by auto-fluorescence from biological samples, and the luminescence from the optical components, which will limit the sensitivity of these biosensors. In the past few years, some investigators use lanthanide complexes with a long lifetime as the biomarker to decrease the background noises in biosensors.[6,7,23,24] Lanthanide complexes have relatively high quantum yields, large stoke shifts, narrow and sharp emission bands, and importantly, their long fluorescence lifetimes (in the order of milliseconds compared with 5–100 ns for conventional fluorophores) allow use of microsecond time-resolved fluorescence measurements, which further reduce the interference of background signals.[25] Unfortunately, the label process of lanthanide complexes linked to aptamers is relatively complicated and expensive, which limits their application in biosensors.

[a]*College of Environmental Science and Engineering, Key Laboratory of Environmental Biology and Pollution Control (Hunan University), Ministry of Education, Hunan University, Changsha 410082, China. E-mail: cgniu@hnu.edu.cn; cgniu@hotmail.com; zgming@hnu.edu.cn; Fax: +86-731-88822829; Tel: +86-731-88823820*
[b]*Hunan University of Science and Engineering, Yongzhou 425100, P. R. China*

† Electronic supplementary information (ESI) available. See DOI: 10.1039/c2an36117e

As one of the very fascinating metallic nanoparticles, gold nanoparticles (GNPs) have attracted many researchers' attention in the last few years, due to their excellent electronic, photonic, magnetic, and optical properties.[26–38] On the basis of the special and strong distance-dependent optical properties, GNPs were usually used as the colorimetric materials in previous academic research.[16–18,28,34,36,37] Commonly, the sensing mechanisms, including crosslinking mechanism[16–18,29–33] and non-crosslinking mechanism,[38,39] are based on GNPs aggregation, which makes the color change from red to blue. The two methods based on GNPs aggregation have the disadvantages of time-consuming (one or two days of assembly) or low sensitivity, respectively. GNPs can quench the fluorescence of organic dyes and quantum dots effectively,[40,41] and the authors found that the GNP is also an efficient quencher for lanthanide complexes.

Considering all this, the authors herein combine the advantages of label-free aptamer, unmodified GNPs and lanthanide complexes to realize a new and sensitive strategy for label-free and time-resolved fluorescence assay of proteins, using Tb-complexes and aptamer-wrapped GNPs. In this protocol, the authors use thrombin as the model analyte to demonstrate the strategy. Human thrombin is used to help control bleeding during surgery.[42] It is necessary to detect thrombin in blood not only for patients suffering from diseases associated with coagulation abnormalities, but also for determining the effectiveness of the therapeutic drugs after surgery or in thromboembolic disease treatments. Hence, the authors herein report a sensitive strategy for thrombin detection in both buffer and human serum. The proposed biosensor exhibited good selectivity and high sensitivity and showed great potential in clinical applications.

2. Experimental section

2.1. Chemicals and apparatus

All oligonucleotides used in the present study were synthesized and HPLC purified by Shanghai Sangon Biological Engineering Technology & Services Co., Ltd. (Shanghai, China) and dissolved in ultrapure water (18.3 MΩ cm) produced by a Millipore water purification system. Their base sequences are as follows: 15-mer thrombin binding aptamer, 5′-GGTTGGTGTGGTTGG-3′; Control random nucleic acid sequence, 5′-AGTTGTAACGGAAGA-3′. Human α-Thrombin (T6884) was purchased from Sigma-Aldrich (Shanghai) Trading Co., Ltd. (Shanghai, China), and stored at −20 °C in PBS buffer containing 50% glycerol. Bovine serum albumin (BSA) was purchased from Sinopharm Chemical Reagent Co., Ltd. (Shanghai, China). Human serum was provided by Hunan University Hospital. $AuCl_3 \cdot HCl \cdot 4H_2O$ was purchased from the Shanghai Institute of Fine Chemical Materials (Shanghai, China). Tb_4O_7 was purchased from Tianjin Guangfu Fine Chemical Research Institute (Tianjin, China). 1,10-Phenanthroline monohydrate (phen) was purchased from Shanghai Shanpu Chemical Co., Ltd. (Shanghai, China). Acetylacetone (AcAc) was purchased from Tianjin Kermel Chemical Reagent Co., Ltd. (Tianjin, China). All other chemicals of analytical grade, were commercially obtained and used without further purification. Ultrapure water was used throughout the experiments. In the present study, the aptamer and control random oligonucleotides were heated at 95 °C for 1 min and then cooled in ice water for 10 min prior to use. The binding buffer was 20 mM Tris–HCl, pH = 7.4, 100 mM NaCl, 1 mM $MgCl_2$, 1 mM $CaCl_2$, and 5 mM KCl.

UV/Vis absorption spectra were recorded by using Shimadzu UV Spectrophotometer (UV-2550, Kyoto, Japan). The time-resolved fluorescence intensities were measured and recorded with a Perkin-Elmer LS-55 spectrofluorimeter (United Kingdom). For time-resolved fluorescence detection, the parameter settings were as follows: excitation wavelength, 311 nm; delay time, 0.1 ms; gate time, 1.0 ms; excitation slit and emission slit, 8.0 nm. The emission intensity was measured at 543 nm. Photographs were taken with a Nikon D 80 digital camera.

2.2. Synthesis of GNPs

All glassware and mechanical stirrers used for the synthesis were thoroughly cleaned in *aqua regia* (3 parts HCl, 1 part HNO_3), rinsed with ultrapure water, and then oven-dried prior to use. The colloidal solution of GNPs synthesized by means of citrate reduction of $AuCl_3 \cdot HCl \cdot 4H_2O$.[43] 5 mL of 38.8 mM sodium citrate was rapidly added to a boiled 50 mL of 1 mM $HAuCl_4$ solution with vigorous stirring in a 250 mL round-bottom flask equipped with a condenser. The color changed from light yellow to wine red. Boiling was continued for 10 min; the heating mantle was then removed, and stirring was continued for an additional 15 min. After the solution was cooled to room temperature, the prepared GNPs solution was stored in the 4 °C refrigerator before use. The size of the nanoparticles was typically ~13 nm in average diameter. The concentration of the GNPs was ~17 nM, which was determined according to Beer's law by using UV/Vis spectroscopy, based on the extinction coefficient of 2.7×10^8 M^{-1} cm^{-1} at $\lambda = 520$ nm for 13 nm particles.[44] The schematic diagram of absorbance spectra of GNPs is shown in the ESI (Fig. S1†).

2.3. Synthesis of $Tb(AcAc)_3phen$

The $Tb(AcAc)_3phen$ using AcAc (Acetylacetone) and phen(1,10-phenanthroline) as the ligands was synthesized according to the literature[45,46] with some modifications. The formula of $Tb(AcAc)_3phen$ is shown in Fig. 1. The details of the synthesis steps are as follows: the terbium ternary complex was prepared by stirring the ethanol solution of phen and AcAc for 10 min (pH was adjusted to 7.0–7.5 by adding sodium hydroxide solution). Subsequently, another ethanol solution of the $TbCl_3$ (Tb_4O_7 was taken in a beaker containing concentrated HCl and H_2O_2; the entire solution was boiled in a water bath and after boiling for 30

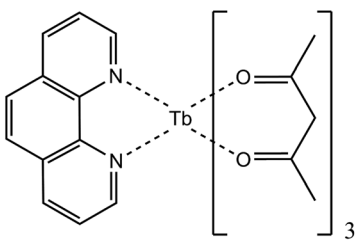

Fig. 1 Structure of complex $Tb(AcAc)_3phen$.

min a clear solution of $TbCl_3$ was obtained, and then the excess HCl and H_2O were removed by heating) was added, and the mixture was stirred for 2.0 h at 78 °C. Finally, white precipitation was obtained and then the white precipitation was filtered, washed and recrystallized using ethanol. The schematic diagram of fluorescence emission spectra excited at 311 nm of Tb-complexes is shown in ESI (Fig. S1†).

2.4. Procedures for thrombin detection

The brief detection of thrombin was realized by following the steps given in Scheme 1. First, 15-mer thrombin binding aptamer solution (90 μL, 2.5×10^{-8} mol L^{-1}) was mixed with different concentrations of thrombin (90 μL) in binding buffer (the control solution without target was obtained by addition of the same volume of buffer), and the mixture was incubated for 45 min at 37 °C to form thrombin–aptamer complex. Second, the GNPs (120 μL) was added to the prepared solution, and the mixture was left for 5 min at room temperature, then 0.5 mol L^{-1} NaCl (20 μL) solution was added to induce the aggregation of GNPs. The resulting mixture was centrifuged (900 rpm for 10 min) to remove the generated GNPs aggregates. Finally, 20 μL supernatant was mixed with 600 μL Tb-complexes (1.0 mg dissolved in 100 mL water), and then pipetted into the cuvette, the time-resolved fluorescence signal was measured and recorded by a Perkin-Elmer LS-55 spectrofluorimeter. For the sensitivity experiment, the concentrations of thrombin were of 0, 0.25, 0.50, 0.75, 1.0, 2.5, 5.0, 7.5, 10.0, 20.0 nM, respectively. For the optimizing experiments of the proposed method, 5.0 nM was selected as the thrombin concentration to determine the optimum experimental conditions. BSA of 100 nM and thrombin of 5.0 nM were used in the selectivity experiment. The concentrations of thrombin detected in human serum were of 0.25, 0.75, 1.0, 7.5 nM, respectively.

3. Results and discussion

3.1. Experimental principle and sensing scheme

GNPs in solution are typically stabilized by adsorbed negative ions (*e.g.*, citrate) whose repulsion prevents the strong van der Waals attraction between gold particles from causing them to aggregate. Ordinarily, exposure to salt screens the repulsive interactions among GNPs with negatively charged coating of citrate ions. The salt can result in the aggregation of GNPs and the solution color changing from red to blue. The aggregated GNPs can be easily centrifuged at low speed. Interestingly, the unstructured aptamer can be effectively adsorbed on the surface of GNPs, and enhance the stability of GNPs in high concentration of salt. However, the stabilization effect was insignificant in the presence of aptamer target. The structured aptamer cannot significantly adsorb on the surface of GNPs, and the GNPs can aggregate easily when high concentration of salt is added to the solution. Hence, the GNPs can effectively differentiate the unfolded and folded aptamer, and what is more, the GNP is an efficient quencher for lanthanide complexes. Based on the abilities of GNPs to differentiate the unfolded and folded aptamer and to quench the fluorescence of lanthanide complexes, the authors herein fabricated a biosensor for highly sensitive and selective detection of thrombin.

The authors employed the 15-mer aptamer of thrombin and one random nucleic acid which have the sequences of GGTTGGTGTGGTTGG and AGTTGTAACGGAAGA as the model and control in this study. The main steps of the assay and the sensing scheme of the proposed biosensor are shown in Scheme 1. In the absence of thrombin, the aptamer is random coil-like in solution, and the unfolded aptamer could adsorb on the surface of GNPs against aggregation at a given high concentration of salt. The dispersed GNPs in the solution can quench the fluorescence of Tb-complexes, and causes the decrease of the fluorescence intensity of Tb-complexes. In the presence of thrombin, the aptamer folded to G-quartet. The folded aptamer cannot stabilize the GNPs at a given high concentration of salt, resulting in the aggregation of the GNPs. After centrifugation at low speed to remove the aggregated GNPs, the quenching capability of the supernatant for Tb-complexes is decreased. Thus, the concentration of thrombin can be detected by monitoring the change of fluorescence intensity of Tb-complexes.

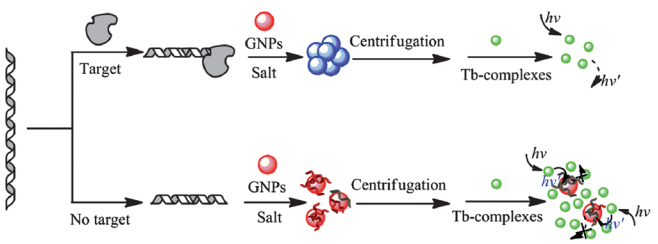

Scheme 1 The schematic diagram of this sensitive detection method. In the presence of thrombin, the aptamer is inclined to form G-quartet, and the folded aptamer cannot adsorb on the surface of GNPs, inducing the GNPs to aggregate in the presence of 0.5 mol L^{-1} salt, the aggregates are discarded after centrifugation. Thus, the mixture solution exhibits strong fluorescence intensity. On the contrary, in the absence of thrombin, the aptamer wraps on the surface of GNPs, making the GNPs well disperse in the solution, resulting in the fluorescence intensity of Tb-complexes decreasing.

3.2. Optimization of the proposed method conditions

Based on the principle of the proposed method, there are two different reaction strategies. In the first one, aptamer and thrombin were mixed firstly, and then the GNPs were added to the mixture. In the second one, aptamer and GNPs were incubated for a while, and then the thrombin was added to the mixed solution. The experimental results indicated that the first strategy showed higher sensitivity than the second one. In the second strategy, the aptamer needs to de-absorb from the GNPs, which increased the difficulty of the molecular recognition process. This may be the reason why the sensitivity in the second strategy is lower. Thus, the authors used the first one strategy as the analytical strategy for thrombin detection. In the present strategy, some factors such as the concentration of aptamer, the amount of GNPs, the incubation time, incubation temperature and the media pH can affect the detection sensitivity of the assay. The optimal concentration of aptamer was investigated. It is worth noting that the concentration of aptamer should be high enough to decrease the free thrombin in solution as much as

possible, and also the concentration of aptamer should be as low as possible to guarantee the detection sensitivity. Five different concentrations of aptamer, 2.5 μM, 0.25 μM, 25 nM, 2.5 nM and 0.25 nM, were employed to optimize the condition. The concentration of 25 nM aptamer presents higher sensitivity and more stable signal than others. It should be the appropriate concentration for thrombin reaction. Thus, the concentration of 25 nM aptamer was used in the following experiments.

The amount of GNPs, a vital parameter for thrombin detection, was studied. Twelve different amounts of GNPs were employed to optimize the amount of GNPs used in the proposed method. The results are recorded in Fig. 2. The amount of GNPs at 120 μL presents a lower noise and higher signal to noise ratio than others. Thus, the amount of GNPs used for all experiments was 120 μL.

Generally, longer incubation time yields more stable fluorescence signal. The fluorescence signal was recorded along with the incubation time increase. The results indicate that the fluorescence signal reached a steady state when the incubation time is 45 min. On the basis of this, all the experiments were carried out for the incubation time of 45 min. Furthermore, the incubation temperature is also an important factor in aptamer–thrombin reaction. The authors investigated two usually used temperatures, 37 °C and room temperature (20–22 °C). The results showed that the incubation time was short at 37 °C. So, 37 °C was selected as the operational temperature for all the experiments. In order to benefit the aptamer–thrombin reaction and aptamer adsorbance onto the surface of GNPs, the media pH for all the experimental steps was 7.4 (Tris–HCl buffer) according to the literature.[4,47]

3.3. Investigation of potential influencing factors on Tb-complexes and GNPs

Some potential influencing factors for the time-resolved fluorescence intensity of Tb-complexes in the present assay were investigated. These results were shown in Fig. S2 and S3,† and indicated that the GNPs can effectively quench the time-resolved fluorescence of Tb-complexes, the ssDNA, thrombin and binding buffer have no effect on the fluorescence intensity of Tb-complexes. Similarly, the effects of ssDNA, thrombin, and binding buffer on the aggregation of GNPs were also studied. The results were recorded and described in Fig. S4† and revealed that the ssDNA can prevent the aggregation of GNPs in high concentration of salt, while the thrombin cannot. The binding buffer cannot lead to the aggregation of GNPs.

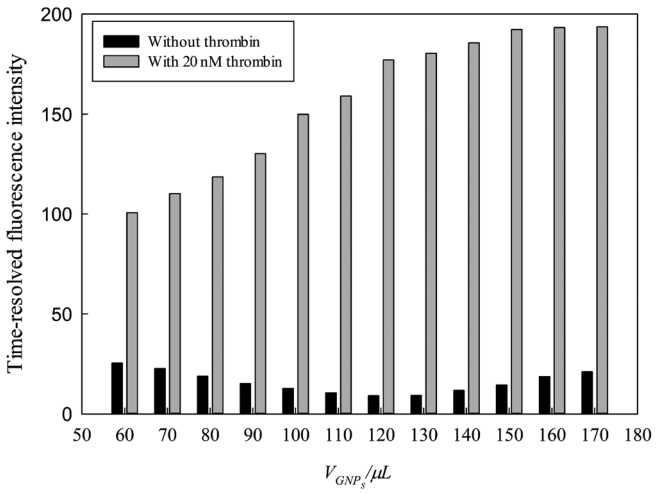

Fig. 2 The optimization of the amount of GNPs used in the present method.

3.4. Detection of thrombin in buffer

Under the optimized assay conditions, the biosensor was employed to detect thrombin in Tris–HCl buffer. Different concentrations of thrombin were added to the buffer and the time-resolved fluorescence emission intensity was measured to evaluate the sensitivity of the biosensor. The different concentrations of thrombin were of 0, 0.25, 0.50, 0.75, 1.0, 2.5, 5.0, 7.5, 10.0, 20.0 nM and the time-resolved fluorescence spectra were recorded at $\lambda_{ex} = 311$ nm, $\lambda_{em} = 543$ nm. The experiment results are shown in Fig. 3. Fig. 3 exhibits the absorption spectra of the supernatant and the time-resolved fluorescence emission spectra of Tb-complexes with the increasing concentrations of thrombin in binding buffer (Tris–HCl, pH = 7.4). The absorption spectra of different supernatants are shown in Fig. 3A. Fig. 3A indicates that as the concentration of thrombin in the solution becomes higher, the absorbance spectra after centrifugation exhibits lower intensity. This is consistent with the fact that higher concentration of thrombin induced more GNPs to aggregate, and less GNPs left in the supernatant. The derived calibration curve is provided as ESI (Fig. S5†). Fig. 3B shows the time-resolved fluorescence emission spectra of aptamer–GNPs–Tb-complexes in different concentrations of thrombin binding buffer. The time-resolved fluorescence emission intensity was significantly increased with the increase of thrombin concentration. This is consistent with the fact shown in Fig. 3A, as the concentration of thrombin in the solution becomes higher, less GNPs are left in the supernatant, and the time-resolved fluorescence intensity is higher. When the concentration of thrombin is lower, the time-resolved fluorescence emission intensity still exhibited perceptible changes. It indicated that the thrombin could be detected with high sensitivity in this proposed sensor.

3.5. Calibration curve of thrombin detection

The time-resolved fluorescence emission intensity was found to be linear with the concentration of thrombin in the range from 1×10^{-9} M to 1×10^{-8} M (Fig. 4). The equation for the resulting calibration plot was $y = 9.709\,x + 37.01$ (x was the concentration of thrombin, y was the time-resolved fluorescence intensity) with correlation coefficient of 0.9777. According to the standard deviation 0.47 for the blank signal with 20 parallel measurements, a limit of detection of approximately 0.14 nM was estimated by three times standard deviation rule. The low limit of detection was sufficient to monitor thrombin changes from basal levels. This value is 71-fold and 14-fold lower than the colorimetric detection of thrombin using unmodified gold nanoparticles and conjugated polyelectrolytes[36] and the aptamer-functionalized GNPs for the amplified optical detection of thrombin.[4] Tb-complexes and GNPs are sensitive probes for

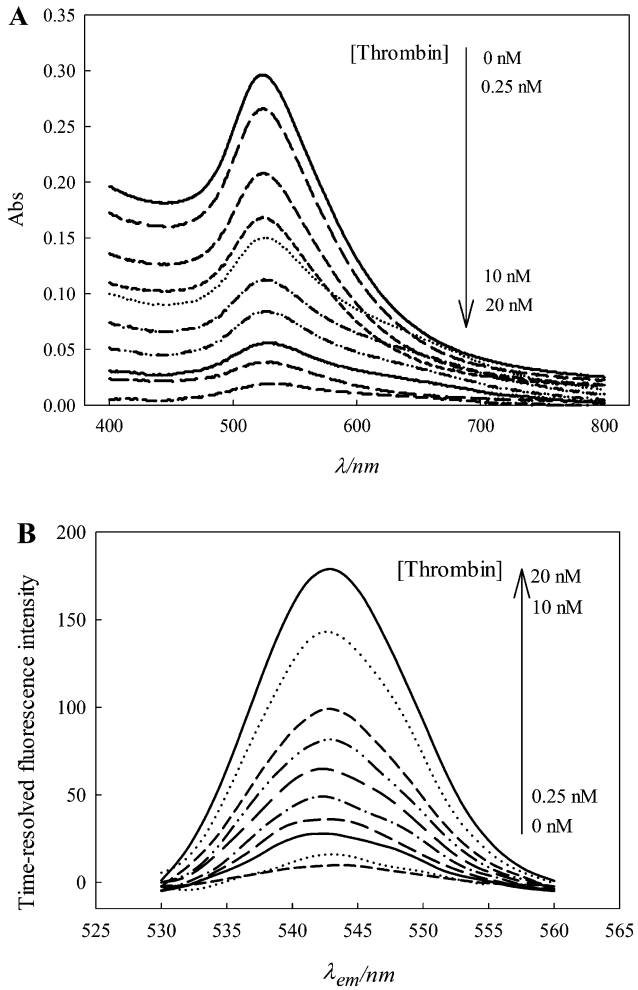

Fig. 3 (A) Absorbance spectra of buffer solutions that include different concentrations of thrombin after the reaction with aptamer and GNPs, followed by the precipitation of the generated aggregates by centrifugation. (B) Time-resolved fluorescence emission spectra for different concentrations of thrombin, for time-resolved spectra: $\lambda_{ex} = 311$ nm, $\lambda_{em} = 543$ nm, delay time, 0.1 ms, gate time, 1.0 ms, excitation slit and emission slit, 8.0 nm.

thrombin detection. The calibration equation can serve as the quantitative basis for the determination of thrombin content in buffer.

3.6. Selectivity for thrombin

In order to evaluate the selectivity of this protocol, the authors conducted some control experiments. The experimental steps were the same as described above. The control experiment results are shown in Fig. 5. The control nucleic acid sequence, which could not form G-quartet structure with thrombin, can make the GNPs stabilize in the presence of thrombin and 0.5 mol L^{-1} salt. The well-dispersed GNPs can cause the fluorescence intensity of Tb-complexes to decrease. The system with BSA at 100 nM also made the fluorescence intensity decrease sharply. However, significant Tb-complexes fluorescence enhancement occurred after the addition of 5.0 nM thrombin and thrombin–BSA mixture (5.0 nM thrombin + 100 nM BSA) to the

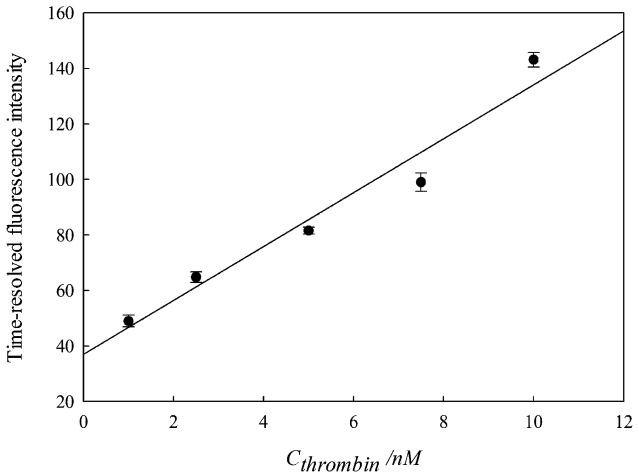

Fig. 4 The linear relationship between the time-resolved fluorescence intensity and thrombin concentration. The concentrations of thrombin were 1.0 nM, 2.5 nM, 5.0 nM, 7.5 nM, 10 nM. Every data point was the mean of three measurements. The error bars are the standard deviation.

solution containing thrombin binding aptamer. These results indicate that the strategy for thrombin detection is selectivity.

3.7. Detection of thrombin in human serum

The practical applicability of the present method was tested by monitoring the thrombin in human serum. Serum is what remains from whole blood after coagulation. Its chemical composition is similar to plasma, but it does not contain coagulation proteins such as thrombin or other composition. Standard solutions of thrombin were added to human serum to test the performance of the sensing system in complex matrixes. The serum sample was spiked with 0.25, 0.75, 1.0, 7.5 nM thrombin. The results are shown in Fig. 6, and the recoveries and the relative standard derivations of 0.25, 0.75, 1.0, 7.5 nM were 90.6%, 96.1%, 88.1%, 103% and 10%, 4.9%, 5.8%, 3.9%,

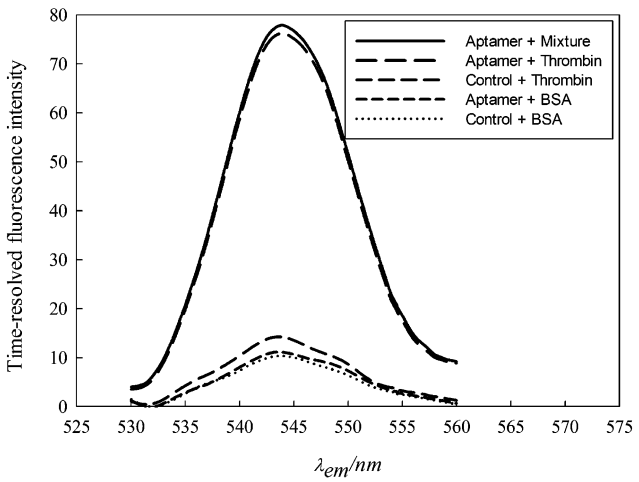

Fig. 5 Time-resolved fluorescence emission spectra for different kinds of mixture solution after centrifugation. The concentrations of aptamer and control random nucleic acid are 2.5×10^{-8} M, and the concentrations of thrombin and BSA are 5.0 nM and 100 nM.

respectively. These results demonstrate that the sensing strategy is also workable in complex matrixes.

4. Conclusion

In summary, a sensitive strategy for thrombin detection is presented. The emission of the Tb-complexes is effectively quenched by gold nanoparticles and the novel strategy is sensitive and selective for thrombin detection by time-resolved fluorescence method. The long lifetime fluorescence of Tb-complexes can easily discriminate from the background signal of complex biological media. Low concentrations of target can be detected without sample pre-treatment. More importantly, this strategy is not only limited to detect thrombin, but also able to detect other targets, which the aptamers predominantly exist as random coils in solution and fold to a well ordered structure in the presence of specific targets. The authors believe that the strategy with good selectivity, high sensitivity and simple processes, may be an alternative method for aptamer-based detection in clinical applications.

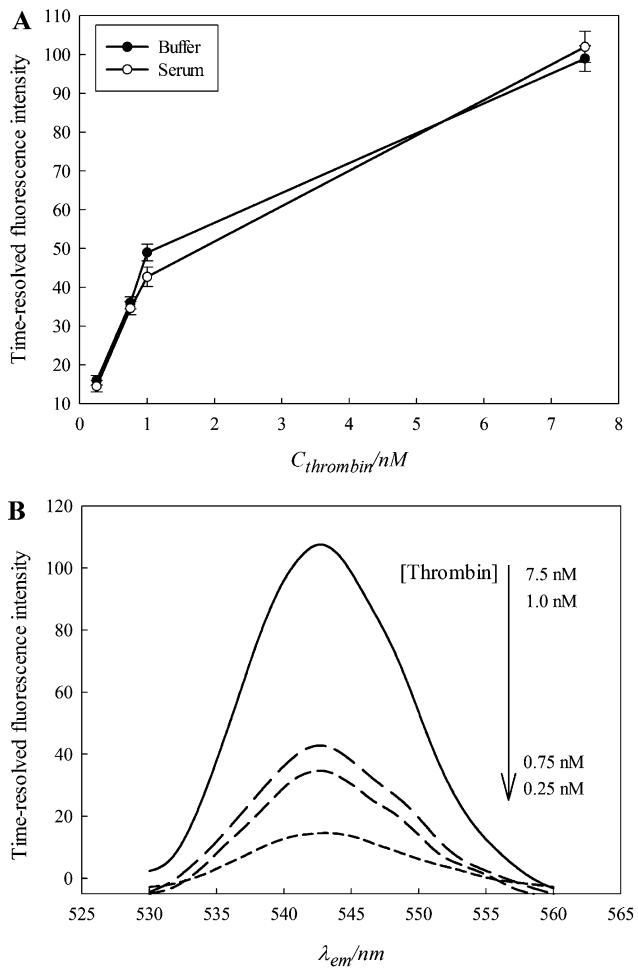

Fig. 6 (A) Results obtained with serum samples spiked with different concentrations of thrombin and comparison with the same concentrations tested in buffer. (B) Time-resolved fluorescence emission spectra of Tb-complexes in human serum with different concentrations of thrombin. The concentrations of thrombin were 0.25 nM, 0.75 nM, 1.0 nM, and 7.5 nM.

Acknowledgements

This work was financially supported by the National Natural Science Foundation of China (20977026, 51039001), the National 863 High Technology Research Foundation of China (2006AA06Z407), the Project-sponsored by SRF for ROCS, SEM (521294018), the Research Fund for the Doctoral Program of Higher Education of China (20090161110009), the Hunan Provincial Natural Science Foundation of China (11JJ2009), and the Fundamental Research Funds for the Central Universities of Hunan University (531107040375).

References

1 A. D. Ellington and J. W. Szostak, *Nature*, 1990, **346**, 818–822.
2 C. Tuerk and L. Gold, *Science*, 1990, **249**, 505–510.
3 J. K. Herr, J. E. Smith, C. D. Medley, D. H. Shangguan and W. H. Tan, *Anal. Chem.*, 2006, **78**, 2918–2924.
4 V. Pavlov, Y. Xiao, B. Shlyahovsky and I. Willner, *J. Am. Chem. Soc.*, 2004, **126**, 11768–11769.
5 N. Tuleuova, C. N. Jones, J. Yan, E. Ramanculov, Y. Yokobayashi and A. Revzin, *Anal. Chem.*, 2010, **82**, 1851–1857.
6 D. W. Huang, C. G. Niu, P. Z. Qin, M. Ruan and G. M. Zeng, *Talanta*, 2010, **83**, 185–189.
7 D. W. Huang, C. G. Niu, G. M. Zeng and M. Ruan, *Biosens. Bioelectron.*, 2011, **29**, 178–183.
8 N. Yildirim, F. Long, C. Gao, M. He, H. C. Shi and A. Z. Gu, *Environ. Sci. Technol.*, 2012, **46**, 3288–3294.
9 Y. Xiao, V. Pavlov, R. Gill, T. Bourenko and I. Willner, *ChemBioChem*, 2004, **5**, 374–379.
10 T. Hermann and D. J. Patel, *Science*, 2000, **287**, 820–825.
11 H. X. Chang, L. H. Tang, Y. Wang, J. H. Jiang and J. H. Li, *Anal. Chem.*, 2010, **82**, 2341–2346.
12 J. Wang, Y. Shan, W. W. Zhao, J. J. Xu and H. Y. Chen, *Anal. Chem.*, 2011, **83**, 4004–4011.
13 Y. L. Cao, R. Yuan, Y. Q. Chai, L. Mao, H. Niu, H. J. Liu and Y. Zhuo, *Biosens. Bioelectron.*, 2012, **31**, 305–309.
14 Z. Z. Zhang and C. Y. Zhang, *Anal. Chem.*, 2012, **84**, 1623–1629.
15 R. Nutiu and Y. Li, *J. Am. Chem. Soc.*, 2003, **125**, 4771–4778.
16 J. W. Liu and Y. Lu, *Anal. Chem.*, 2004, **76**, 1627–1632.
17 J. W. Liu and Y. Lu, *Anal. Chem.*, 2004, **76**, 1627; J. W. Liu and Y. Lu, *Angew. Chem., Int. Ed.*, 2006, **45**, 90–94.
18 S. J. Chen, Y. F. Huang, C. C. Huang, K. H. Lee, Z. H. Lin and H. T. Chang, *Biosens. Bioelectron.*, 2008, **23**, 1749–1753.
19 Y. Z. Liu, Z. T. Wu, G. H. Zhou, Z. K. He, X. D. Zhou, A. G. Shen and J. M. Hu, *Chem. Commun.*, 2012, **48**, 3164–3166.
20 H. Q. Wang, Z. Wu, L. J. Tang, R. Q. Yu and J. H. Jiang, *Nucleic Acids Res.*, 2011, **39**, e122.
21 A. R. Ruslinda, V. Penmatsa, Y. Ishii, S. Tajima and H. Kawarada, *Analyst*, 2012, **137**, 1692–1697.
22 S. Niu, L. Qu, Q. Zhang and J. Lin, *Anal. Biochem.*, 2012, **421**, 362–367.
23 P. Lode, J. Rosenberg, K. Pettersson and H. Takalo, *Anal. Chem.*, 2003, **75**, 3193–3201.
24 X. Y. Ouyang, R. Q. Yu, J. Y. Jin, J. S. Li, R. H. Yang, W. H. Tan and J. L. Yuan, *Anal. Chem.*, 2011, **83**, 782–789.
25 K. Binnemans, *Chem. Rev.*, 2009, **109**, 4283–4374.
26 E. Katz and I. Willner, *Angew. Chem., Int. Ed.*, 2004, **43**, 6042–6108.
27 H. X. Li and L. Rothberg, *J. Am. Chem. Soc.*, 2004, **126**, 10958–10961.
28 H. X. Li and L. Rothberg, *Proc. Natl. Acad. Sci. U. S. A.*, 2004, **101**, 14036–14039.
29 E. Oh, M. Hong, D. Lee, S. Nam, H. C. Yoon and H. Kim, *J. Am. Chem. Soc.*, 2005, **127**, 3270–3271.
30 N. L. Rosi and C. A. Mirkin, *Chem. Rev.*, 2005, **105**, 1547–1562.
31 K. E. Sapsford, L. Berti and I. L. Medintz, *Angew. Chem., Int. Ed.*, 2006, **45**, 4562–4588.
32 C. S. Thaxton, D. G. Georganopoulou and C. A. Mirkin, *Clin. Chim. Acta*, 2006, **363**, 120–126.
33 N. C. Tansil and Z. Gao, *Nano Today*, 2006, **1**, 28–37.
34 H. Wang, Y. X. Wang, J. Y. Jin and R. H. Yang, *Anal. Chem.*, 2008, **80**, 9021–9028.

35 Z. Q. Tan, J. F. Liu, R. Liu, Y. G. Yin and G. B. Jiang, *Chem. Commun.*, 2009, 7030–7032.
36 F. Xia, X. Zuo, R. Yang, Y. Xiao, D. Kang, A. Vallée-Bélisle, X. Gong, J. D. Yuen, B. B. Y. Hsu, A. J. Heeger and K. W. Plaxco, *Proc. Natl. Acad. Sci. U. S. A.*, 2010, **107**, 10837–10841.
37 P. L. He, L. Shen, R. Y. Liu, Z. P. Luo and Z. Li, *Anal. Chem.*, 2011, **83**, 6988–6995.
38 W. Zhao, W. Chiuman, M. A. Brook and Y. Li, *ChemBioChem*, 2007, **8**, 727–731.
39 L. Wang, X. Liu, X. Hu, S. Song and C. Fan, *Chem. Commun.*, 2006, 3780–3782.
40 Y. Jin, H. Li and J. Bai, *Anal. Chem.*, 2009, **81**, 5709–5715.
41 G. Mandal, M. Bardhan and T. Ganguly, *J. Phys. Chem. C*, 2011, **115**, 20840–20848.
42 D. J. Cada, T. Levien and D. E. Baker, *Hosp. Pharm.*, 2008, **43**, 577–585.
43 C. G. Katherine, R. G. Freeman, B. H. Michael and J. N. Michael, *Anal. Chem.*, 1995, **67**, 735–743.
44 W. Haiss, N. T. K. Thanh, J. Aveyard and D. G. Fernig, *Anal. Chem.*, 2007, **79**, 4215–4221.
45 L. R. Melby, N. J. Rose, E. Abramson and J. C. Caris, *J. Am. Chem. Soc.*, 1964, **86**, 5117–5125.
46 H. Chen and W. G. Zhang, *J. Am. Ceram. Soc.*, 2010, **93**, 2305–2310.
47 L. P. Sun, J. F. Zhang, H. Li, X. Y. Wang, Z. W. Zhang, S. Wang and Q. Q. Zhang, *Chem. J. Chin. Unvi.*, 2009, **30**, 95–99.